

# The effect of the molecular structures of dicyanomethylene compounds on their supramolecular assembly, photophysical and electrochemical properties

Catiúcia R. M. O. Matos,<sup>a</sup> Fábio S. Miranda,<sup>a</sup> José W. M. Carneiro,<sup>a</sup>  
Carlos B. Pinheiro,<sup>b</sup> Célia M. Ronconi<sup>\*a</sup>

<sup>a</sup> Instituto de Química, Universidade Federal Fluminense, Outeiro de São João Batista, s/n, Campus do Valongo, Centro, 24.020-141, Niterói, RJ, Brazil

<sup>b</sup> Departamento de Física, ICEX, Universidade Federal de Minas Gerais, Av. Antônio Carlos 6627 Pampulha, CEP 31270-901, Belo Horizonte, MG, Brazil

E-mail:[cmronconi@id.uff.br](mailto:cmronconi@id.uff.br)

## Supporting Information

Fourier transform infrared and  $^1\text{H}$  and  $^{13}\text{C}$  NMR spectra of the synthesized compounds

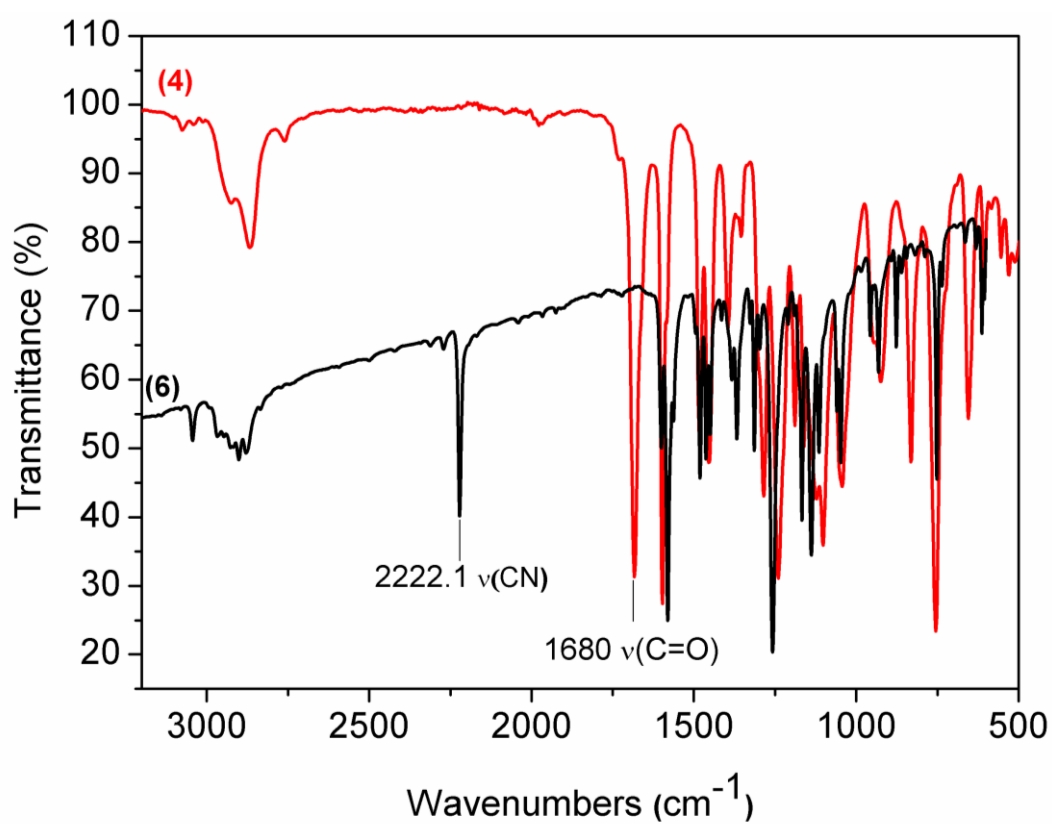
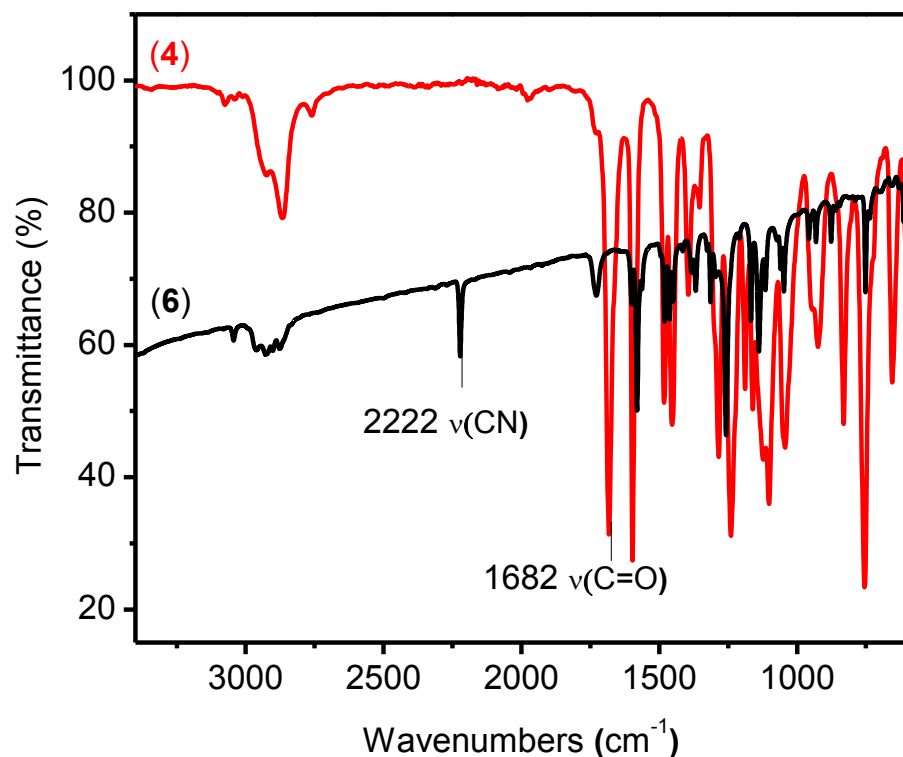
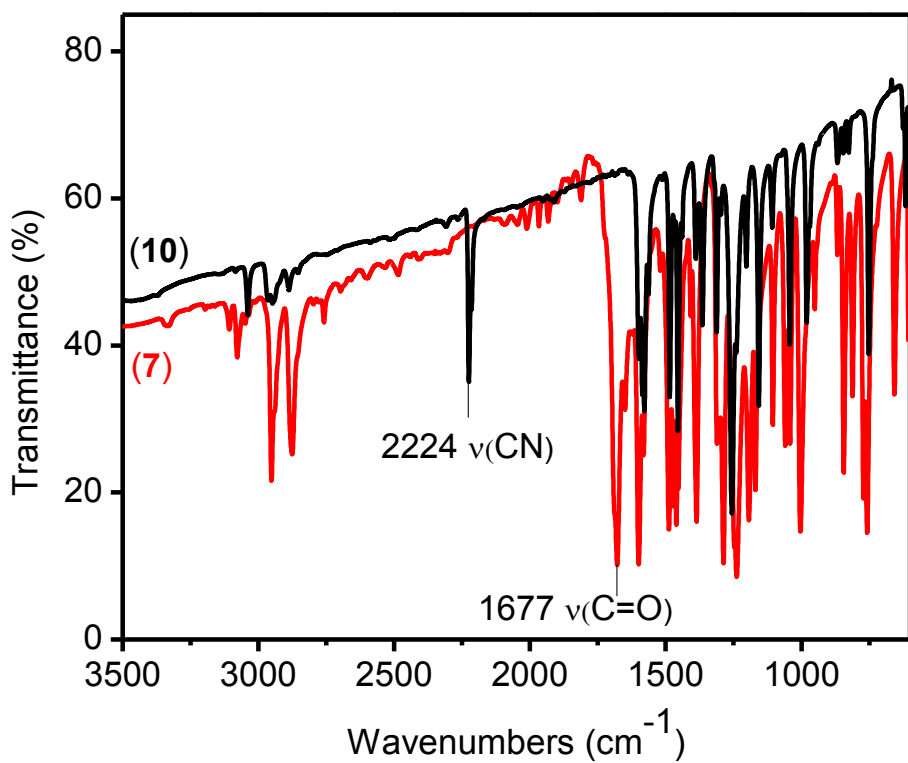


Fig. S1 IR spectra of compounds (3) and (5).



**Fig. S2** IR spectra of compounds (4) and (6).



**Fig. S3** IR spectra of compounds (7) and (10).

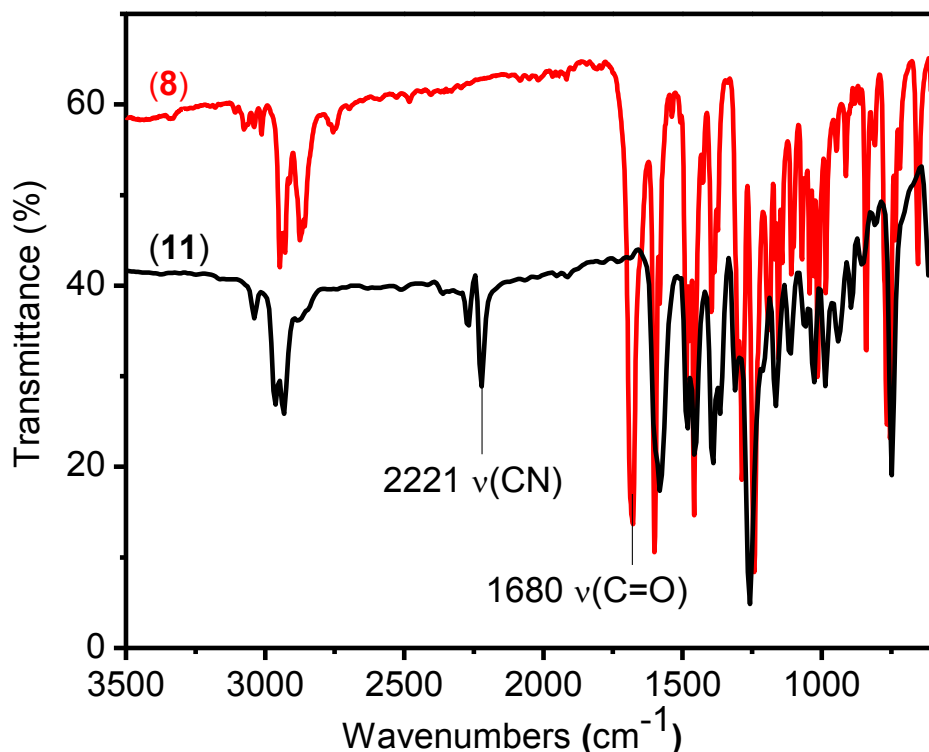


**Fig. S4** IR spectra of compounds (8) and (11).

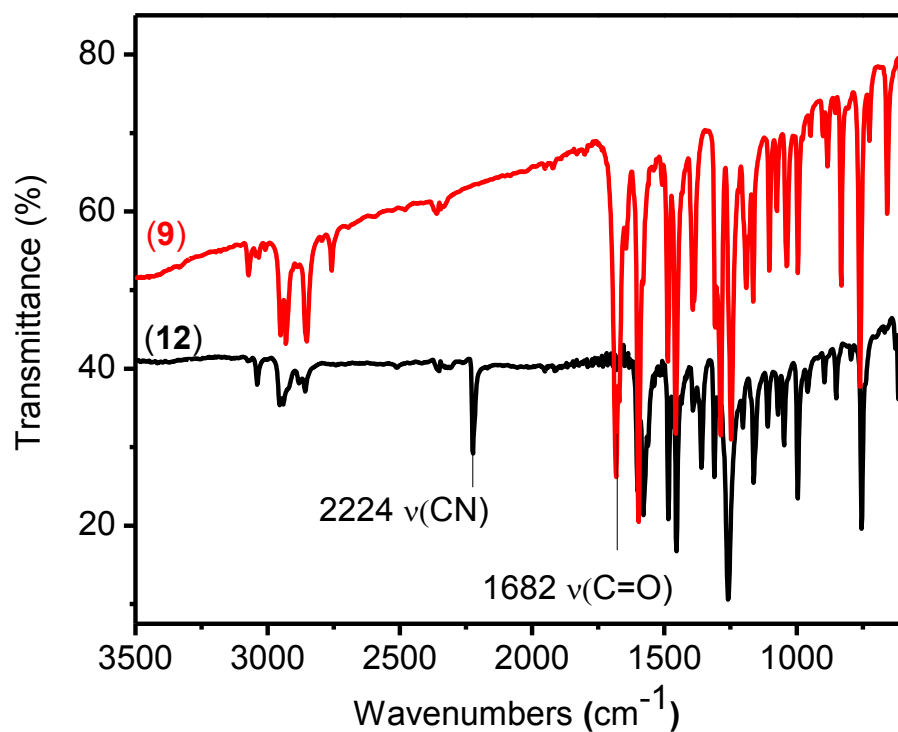


**Fig. S5** IR spectra of compounds (9) and (12).

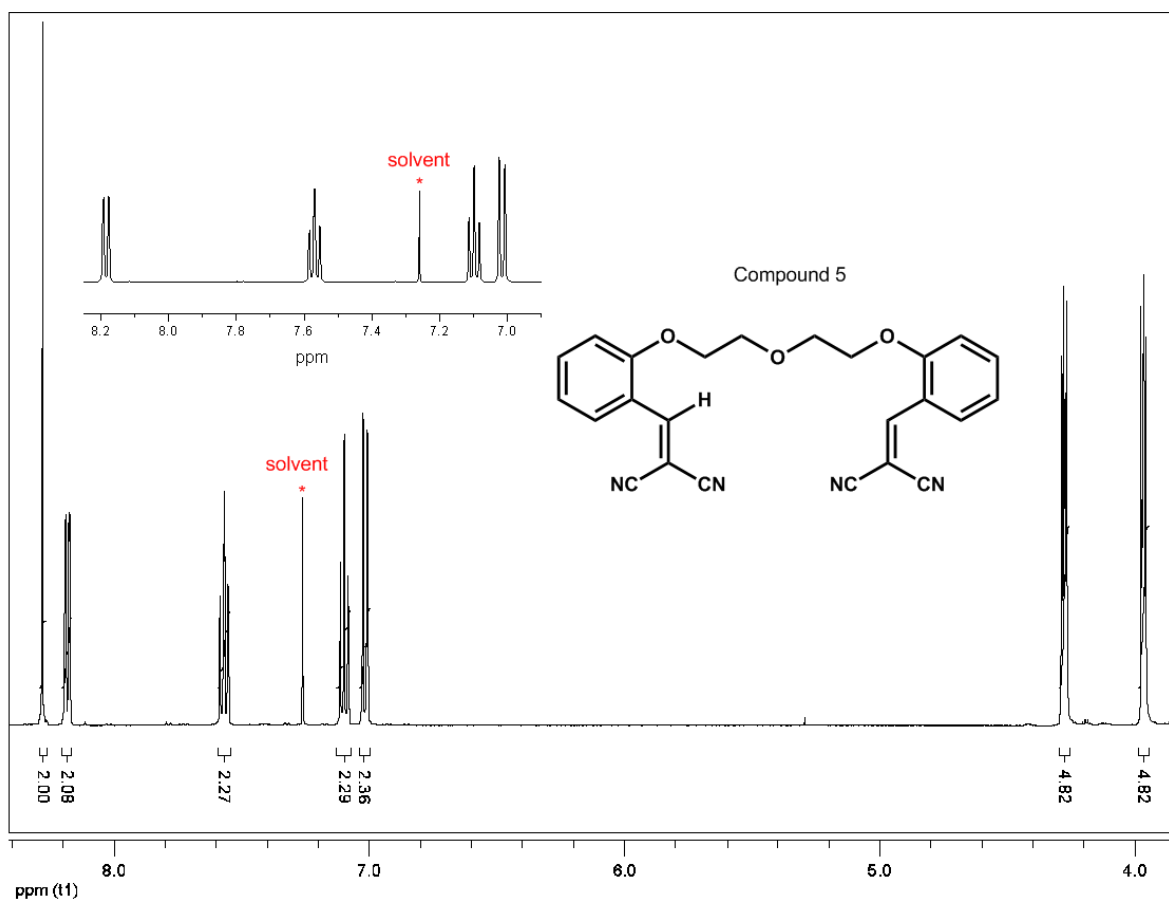


**Fig. S6**  $^1\text{H}$  NMR spectrum of compound (**5**) (500 MHz, 298K,  $\text{CDCl}_3$ ).

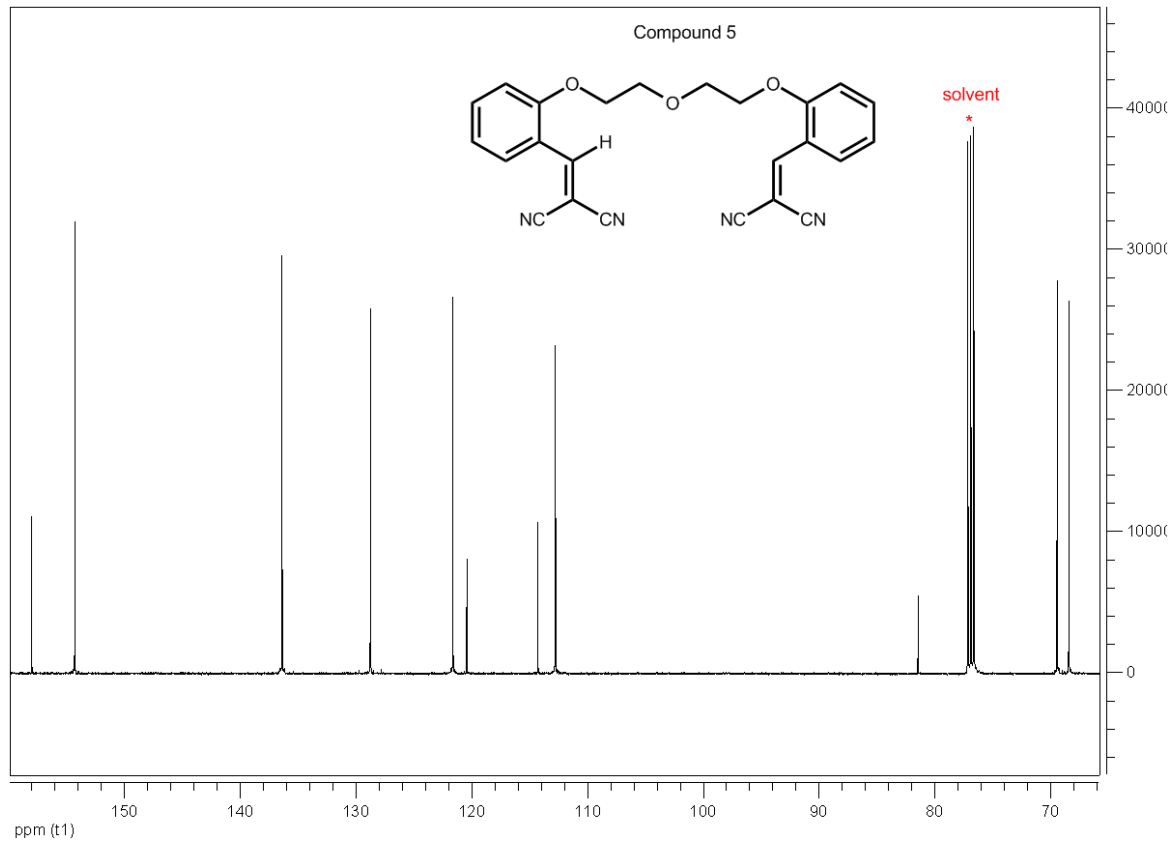


**Fig. S7**  $^{13}\text{C}$  NMR spectrum of compound (5) (125 MHz, 298K,  $\text{CDCl}_3$ ).

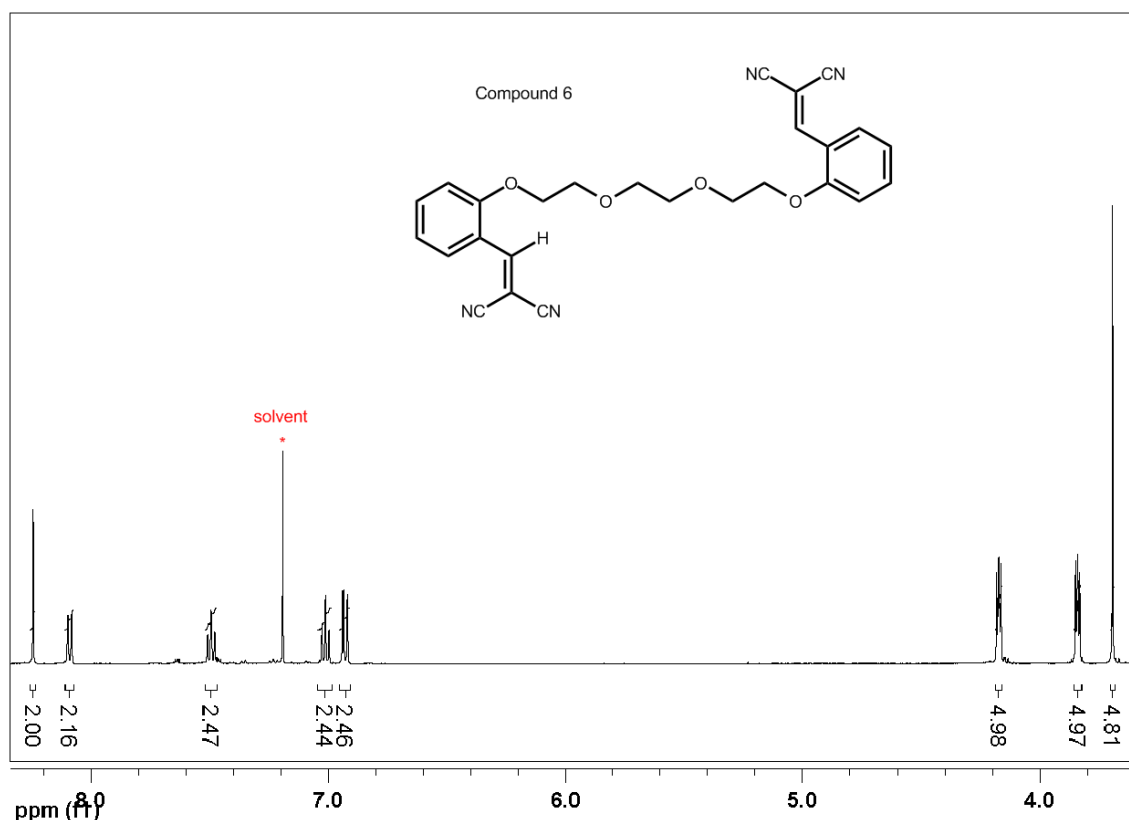


**Fig. S8**  $^1\text{H}$  NMR spectrum of compound (6) (500 MHz, 298K,  $\text{CDCl}_3$ ).

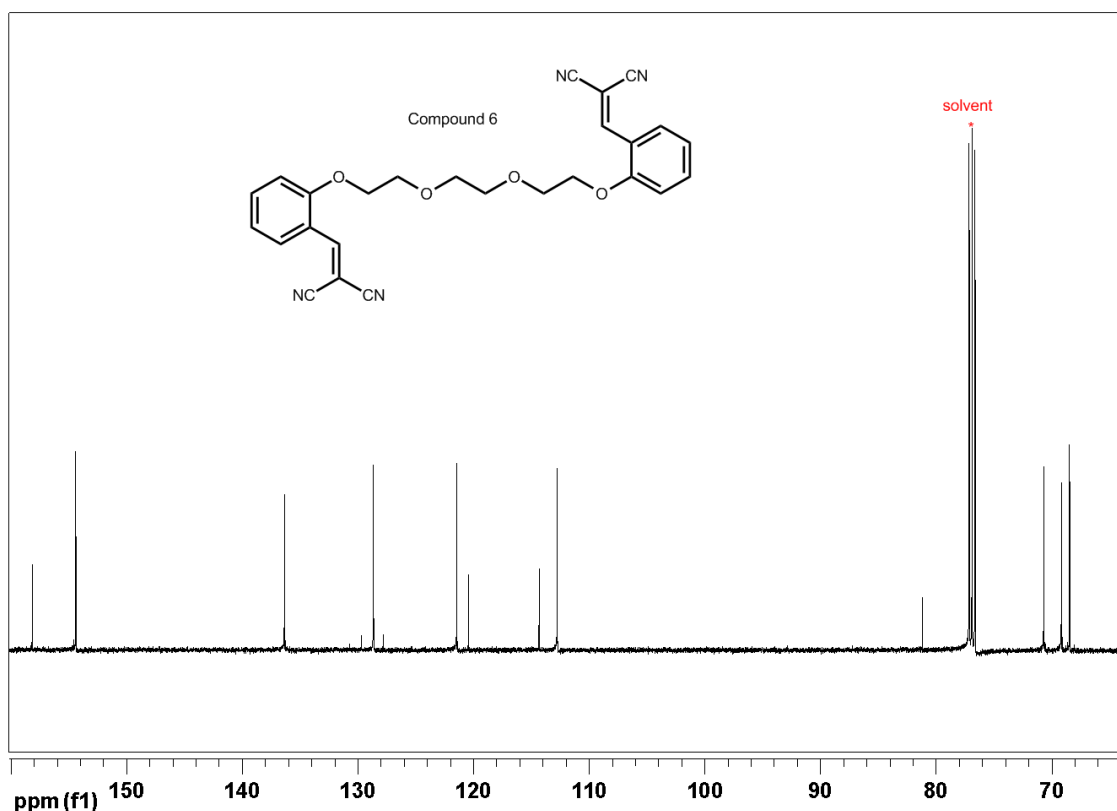


**Fig. S9**  $^{13}\text{C}$  NMR spectrum of compound (6) (125 MHz, 298K,  $\text{CDCl}_3$ ).

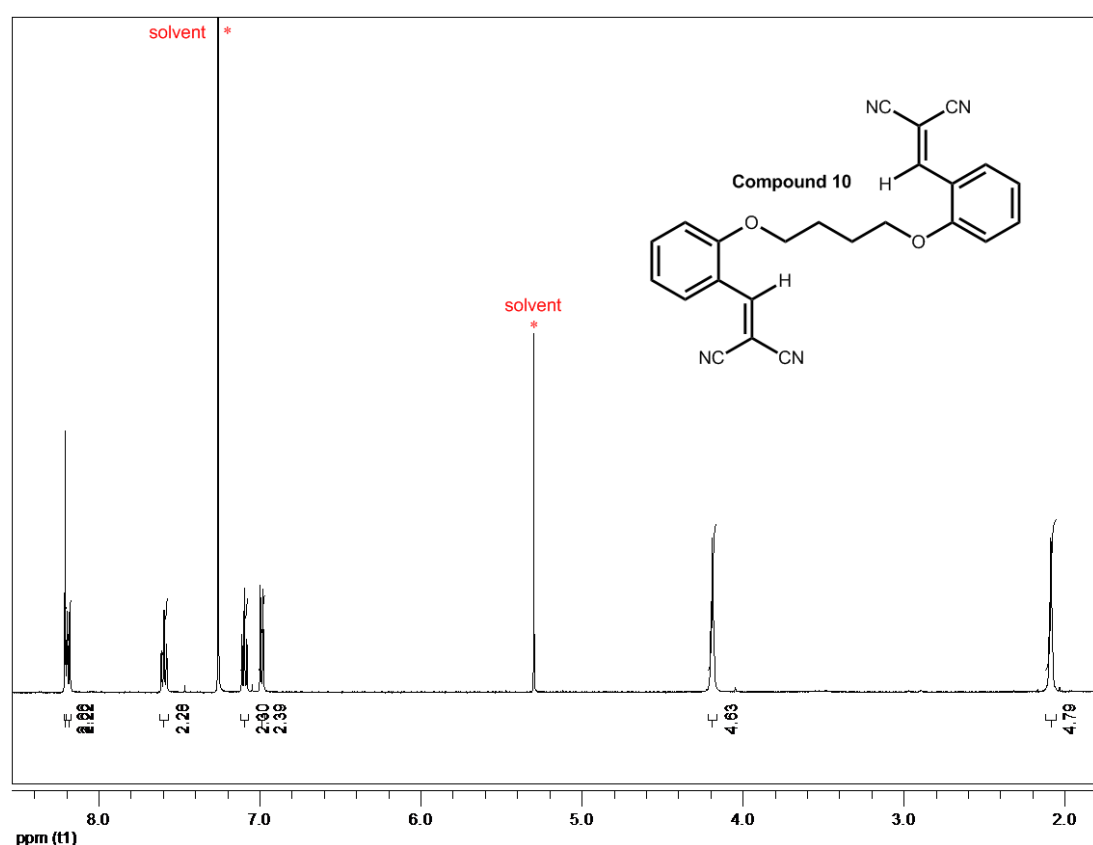


**Fig. S10**  $^1\text{H}$  NMR spectrum of compound (10) (500 MHz, 298K,  $\text{CDCl}_3$ ).

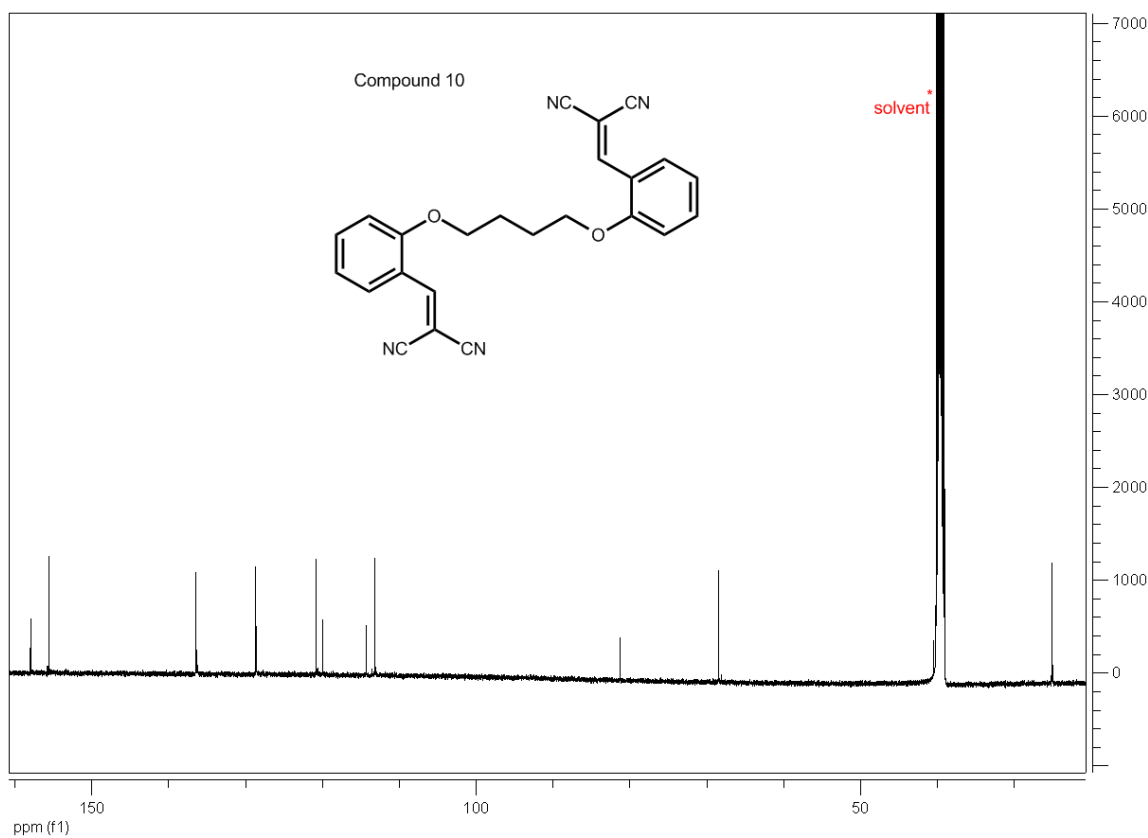


**Fig. S11** <sup>13</sup>C NMR spectrum of compound (**10**) (125 MHz, 298K, DMSO).

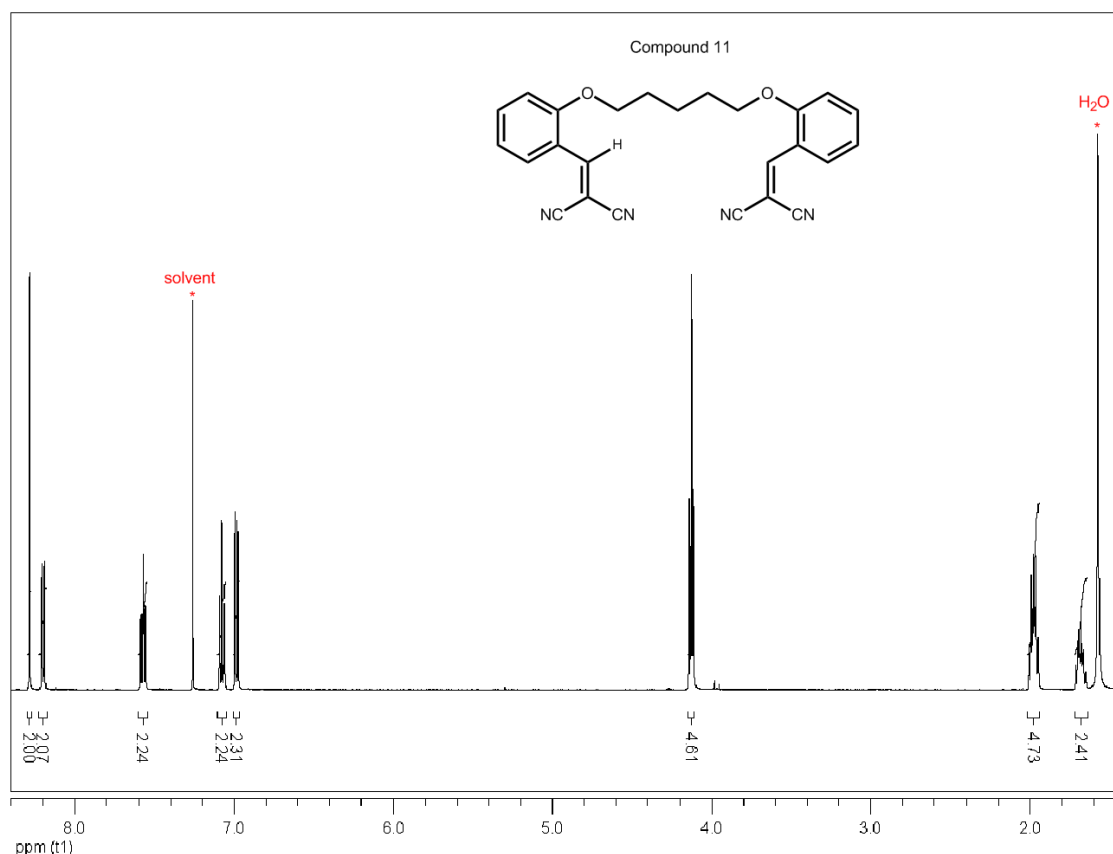


**Fig. S12** <sup>1</sup>H NMR spectrum of compound (**11**) (500 MHz, 298K, CD<sub>3</sub>Cl).

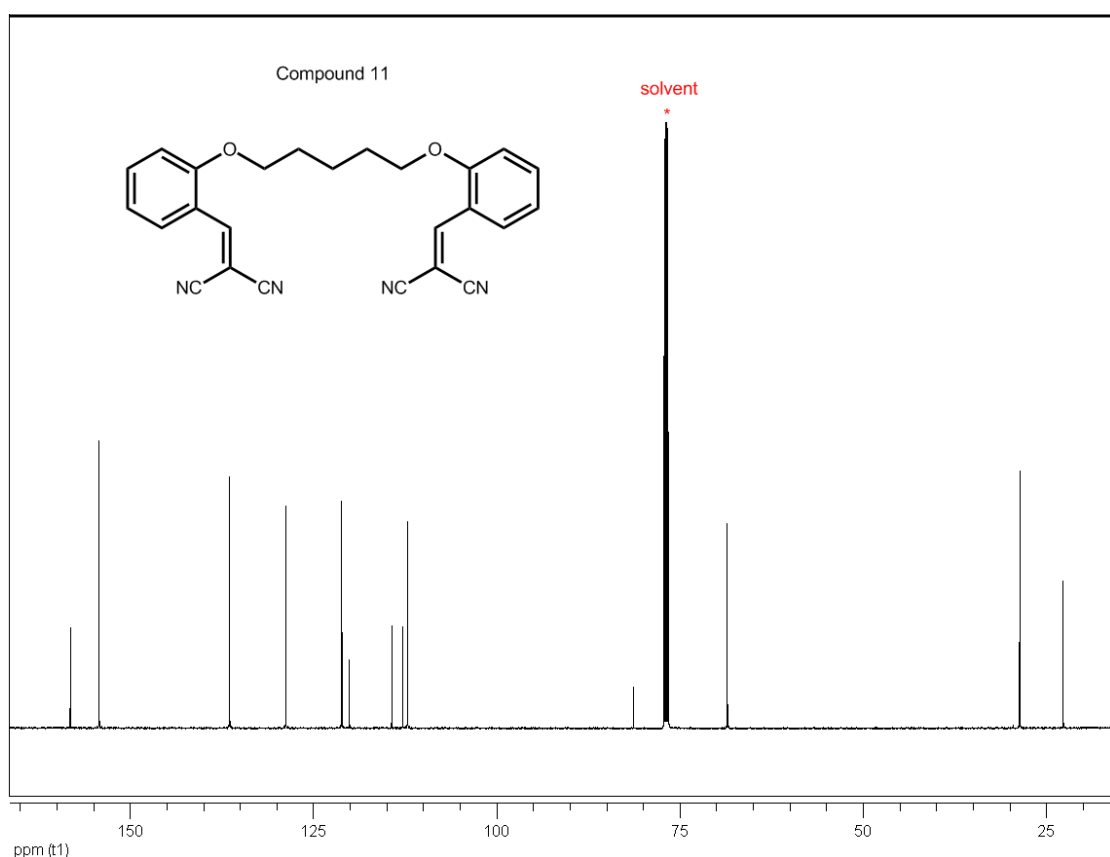


**Fig. S13** <sup>13</sup>C NMR spectrum of compound (**11**) (125 MHz, 298K, CDCl<sub>3</sub>).

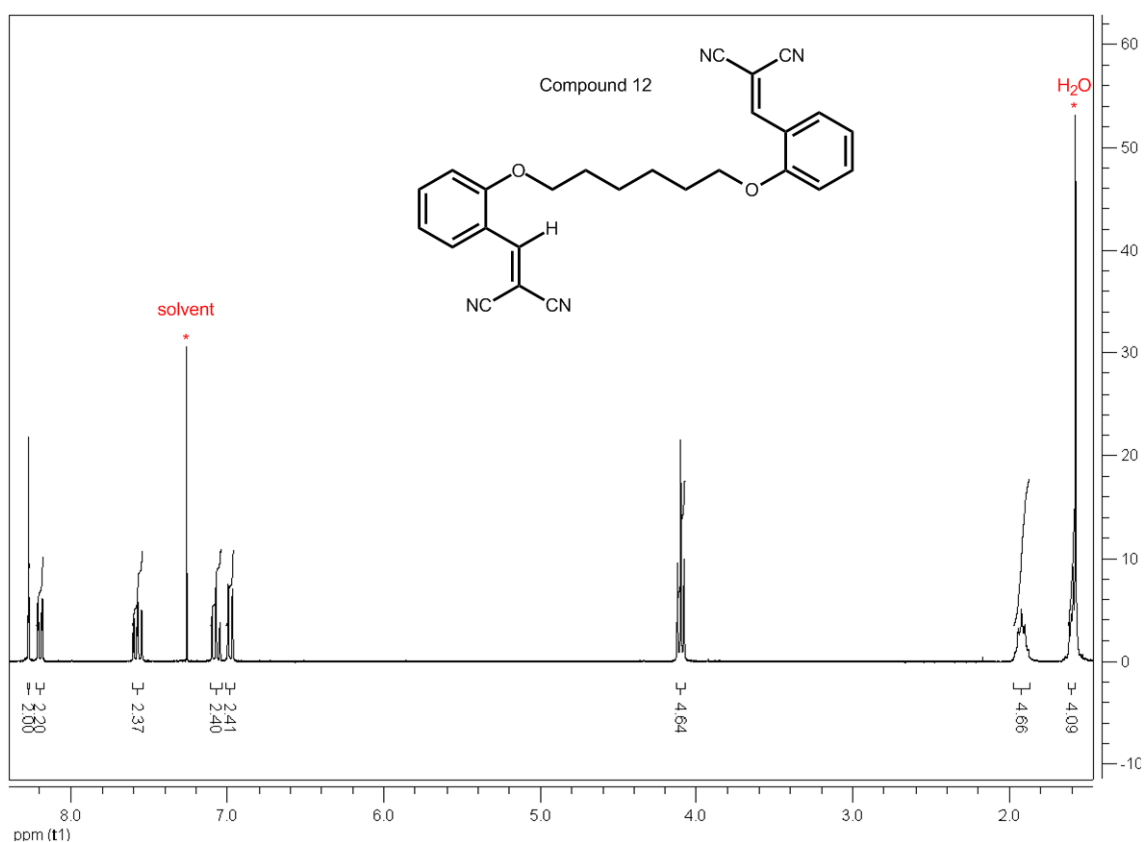


**Fig. S14** <sup>1</sup>H NMR spectrum of compound (**12**) (500 MHz, 298K, CDCl<sub>3</sub>).

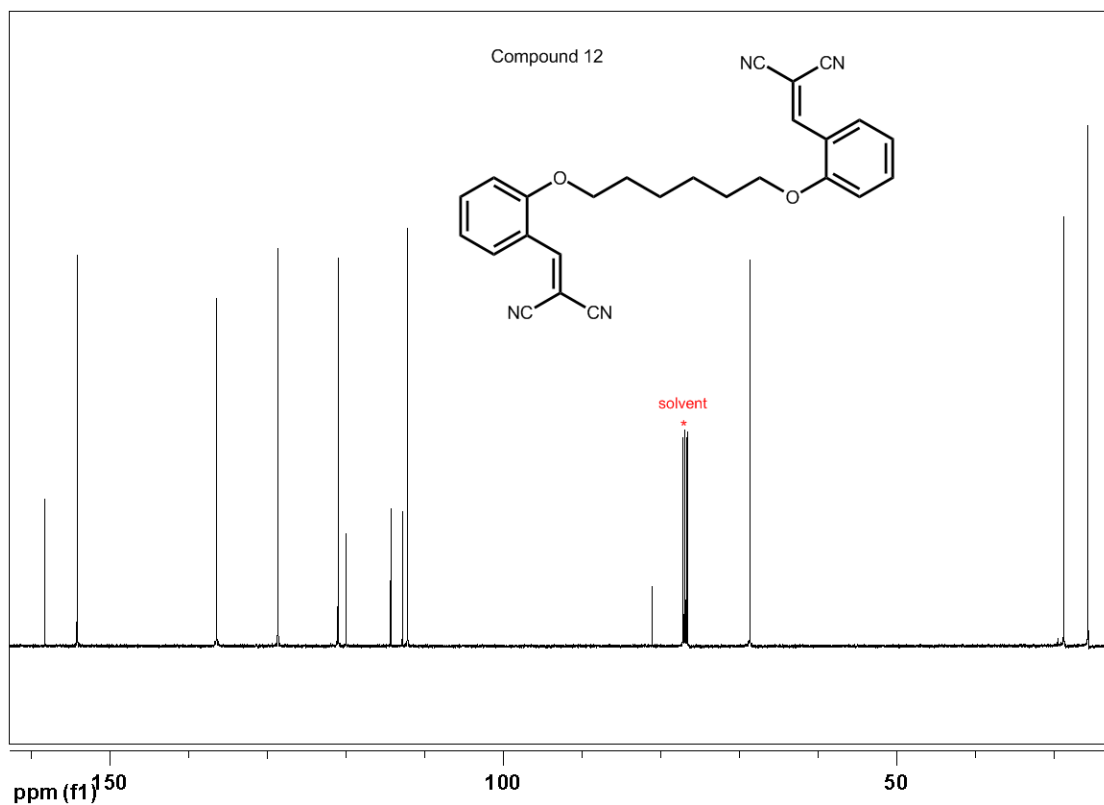


**Fig. S15**  $^{13}\text{C}$  NMR spectrum of compound (**12**) (125 MHz, 298K,  $\text{CDCl}_3$ ).

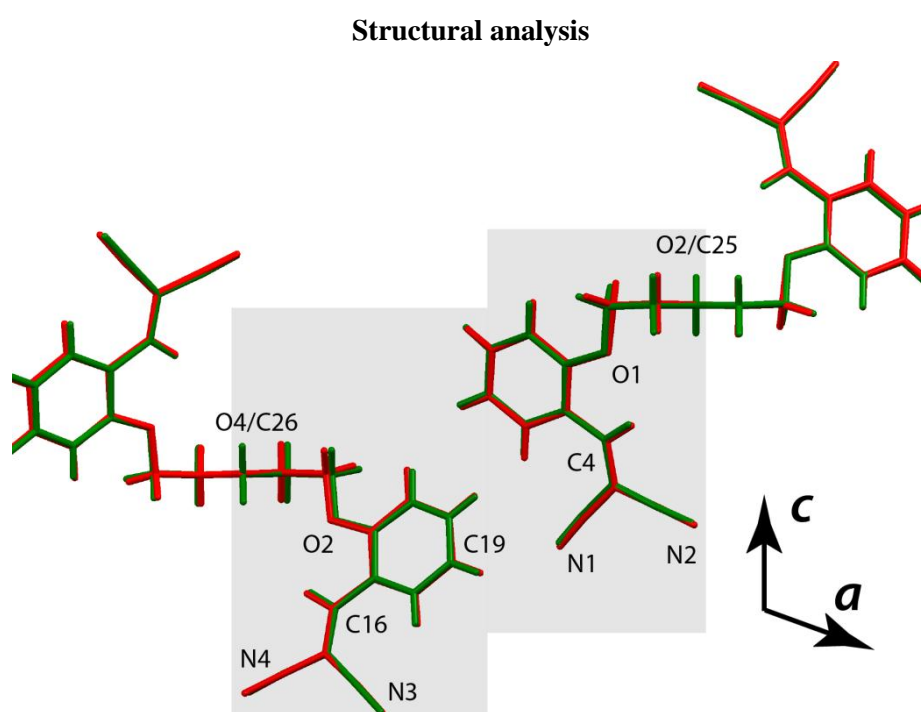


**Fig. S16** Overlay of the structures of compounds **5** (red) and **11** (green) in which the grey area highlights the asymmetric unit. Relevant atoms for the structure packing are indicated.

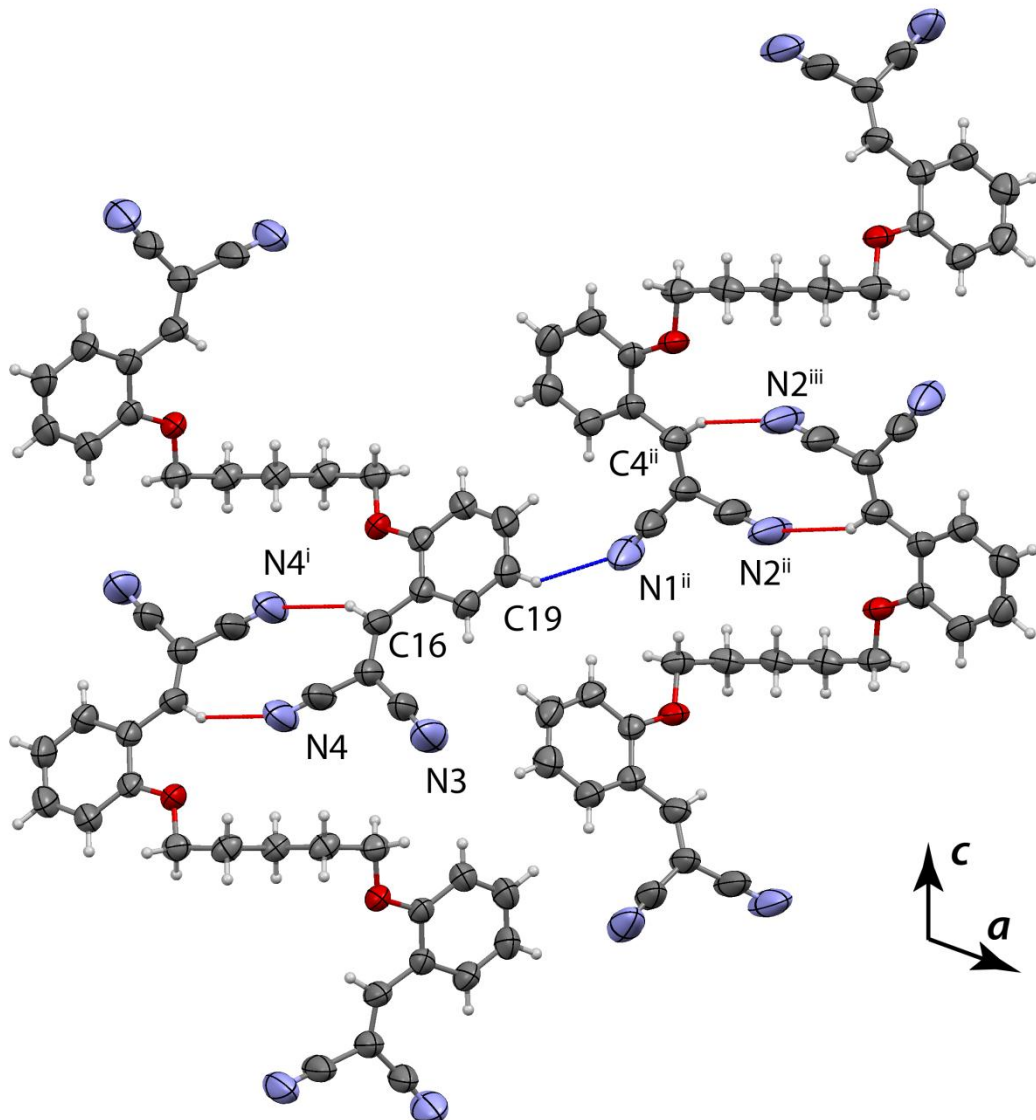


**Fig. S17** Packing representation of compound **11**. Oxygen atoms indicated in red. C-H...N (red links) and C...N (blue links) weak hydrogen bonds connecting molecules ( $i = 1-x, -1-y, 1-z$ ;  $ii = x, -1+y, z$ ;  $iii = 1-x, -1-y, 1-z$ ).

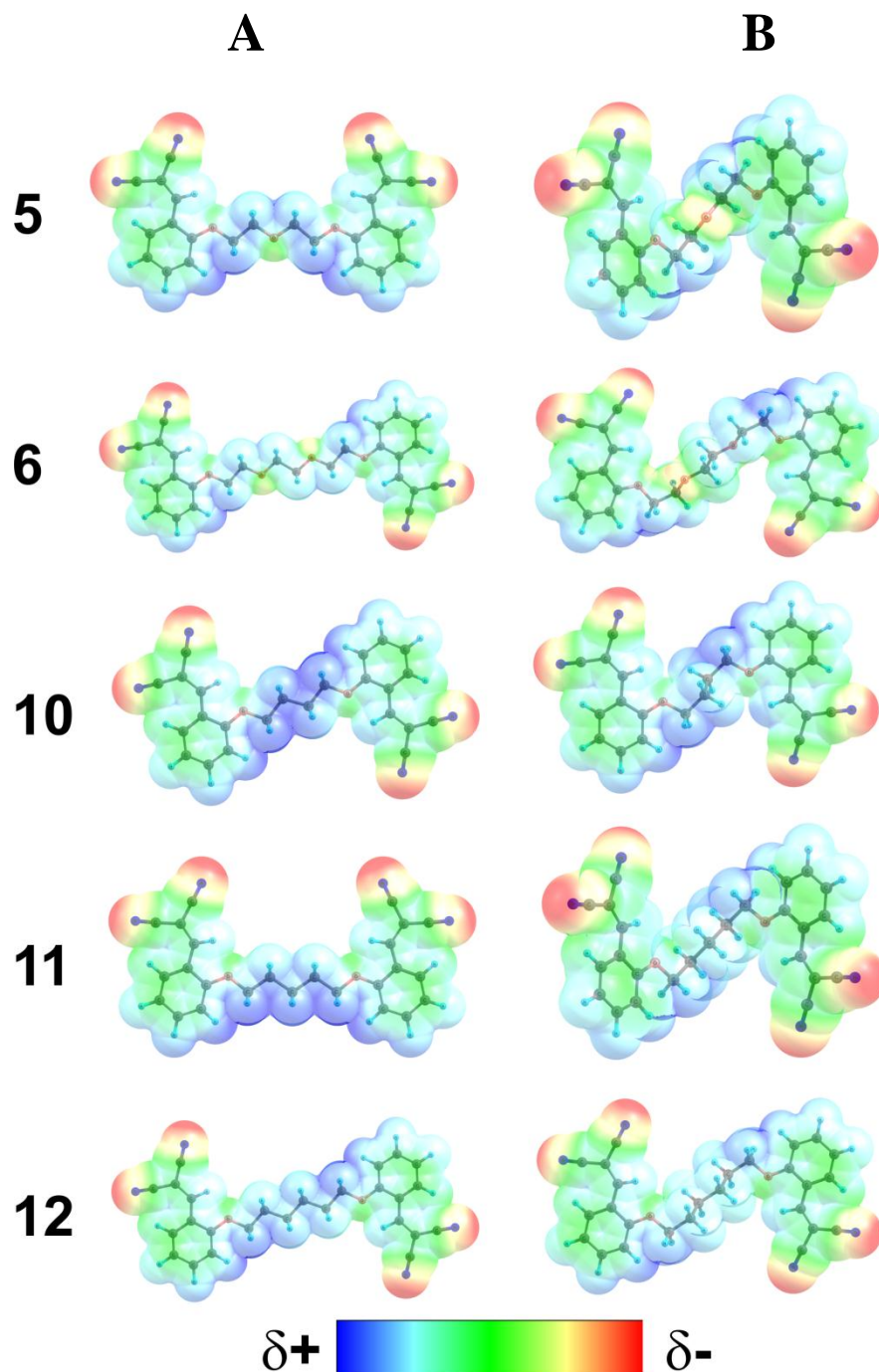


**Fig. S18** Electrostatic potential surfaces for (A) the fully planar structures with zig-zag arrangement of the spacers and (B) for the structures obtained from CIF files.

**Cyclic voltammetry**

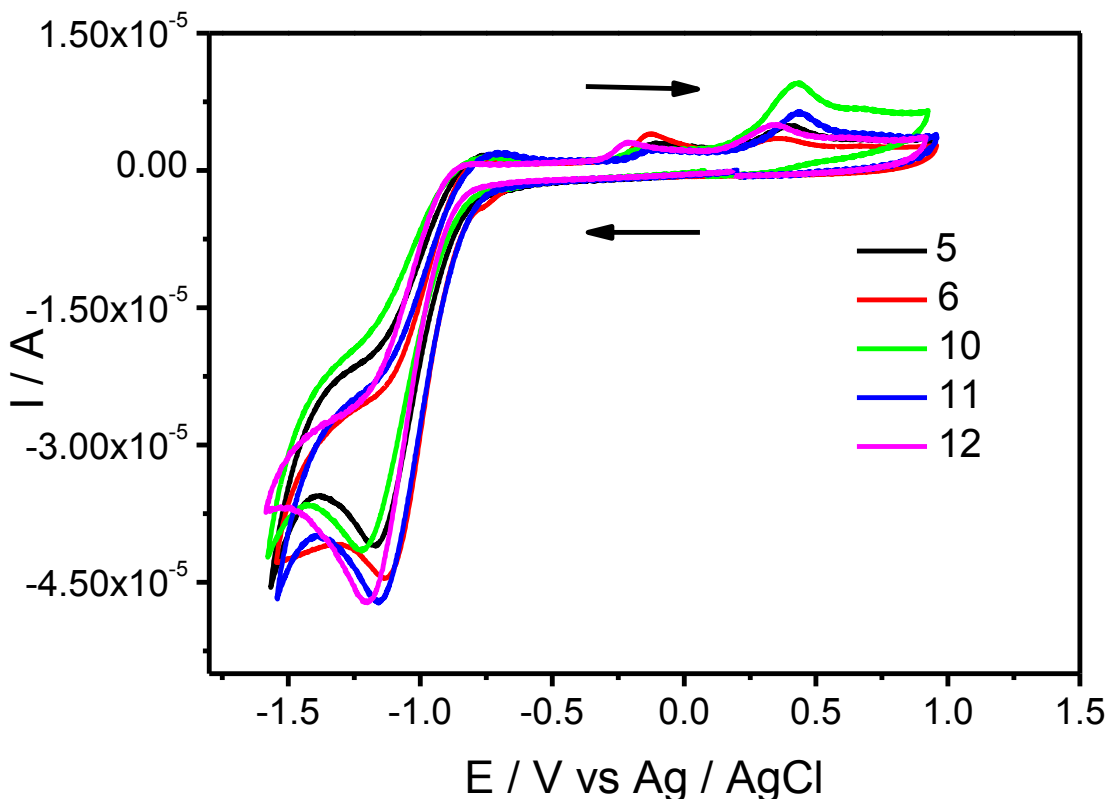


**Fig. S19** The cyclic voltammograms of **5**, **6**, **10**, **11** and **12** in  $0.1 \text{ mol.L}^{-1}$  TBAClO<sub>4</sub>/CH<sub>2</sub>Cl<sub>2</sub> at a scan rate of  $100 \text{ m.V.s}^{-1}$ .

### DFT results

**Table S1** Thermodynamic properties for the equilibrium between the structures obtained from CIF files and fully planar structures with zig-zag arrangement of the spacers, calculated at B3LYP/6-31G(d,p)/PCM(CH<sub>2</sub>Cl<sub>2</sub>).

	<b>5</b>	<b>6</b>	<b>10</b>	<b>11</b>	<b>12</b>
$\Delta H_g^*$	-2.01	-1.40	-1.26	-1.86	-0.99
$\Delta G_g^*$	-0.77	-1.05	0.29	-0.69	0.33
$\Delta S_g^*$	-4.17	-1.17	-5.20	-3.91	-4.45
$\Delta G_{\text{sol}}^*$	-1.06	-1.76	0.91	0.51	1.02

$\Delta$  (Torsion [Based on X-ray structure] – Planar); (\*) corresponds to the process (ideal gas,  $1 \text{ mol.L}^{-1}$ )  $\rightarrow$  (ideal dilute solution,  $1 \text{ mol.L}^{-1}$ ).<sup>1,2</sup>

**Table S2** Thermodynamic properties for the equilibrium between the structures obtained from CIF files and fully planar structures with zig-zag arrangement of the spacers, calculated at B3LYP/6-31+G(d,p)/PCM(CH<sub>2</sub>Cl<sub>2</sub>).

	<b>5</b>	<b>6</b>	<b>10</b>	<b>11</b>	<b>12</b>
$\Delta H_g^*$	-1.84	-1.21	-1.01	-1.71	-0.83
$\Delta G_g^*$	-0.46	-1.10	-0.06	-1.47	-1.29
$\Delta S_g^*$	-4.63	-0.39	-3.21	-0.80	1.57
$\Delta G_{sol}^*$	-0.95	-2.04	0.60	-0.20	-0.50

$\Delta$  (Torsion [Based on X-ray structure] – Planar); (\*) corresponds to the process (ideal gas, 1 mol.L<sup>-1</sup>) → (ideal dilute solution, 1 mol.L<sup>-1</sup>).

**Table S3** Thermodynamic properties for the equilibrium between the structures obtained from CIF files and fully planar structures with zig-zag arrangement of the spacers, calculated at B3LYP/6-31+G(d,p)/PCM(CH<sub>2</sub>Cl<sub>2</sub>).

	<b>5</b>	<b>6</b>	<b>10</b>	<b>11</b>	<b>12</b>
$\Delta H_g^*$	0.58	-9.07	-0.62	-10.41	-9.83
$\Delta G_g^*$	2.26	-8.07	0.29	-10.87	-8.91
$\Delta S_g^*$	-5.64	-3.36	-3.07	1.52	-3.09
$\Delta G_{sol}^*$	-0.13	-0.57	0.57	-0.94	1.01

$\Delta$  (Torsion [Based on X-ray structure] – Planar); (\*) corresponds to the process (ideal gas, 1 mol.L<sup>-1</sup>) → (ideal dilute solution, 1 mol.L<sup>-1</sup>).

**Table S4** Thermodynamic properties for the equilibrium between the structures obtained from CIF files and fully planar structures with zig-zag arrangement of the spacers,, calculated at B3LYP/6-31+G(d,p)/(Vacuum).

	<b>5</b>	<b>6</b>	<b>10</b>	<b>11</b>	<b>12</b>
$\Delta H_g^*$	0.16	1.27	-0.51	-1.08	0.11
$\Delta G_g^*$	0.83	1.52	-0.18	-0.81	0.89
$\Delta S_g^*$	-2.26	-0.83	-1.11	-0.91	-2.63

$\Delta$  (Torsion [Based on X-ray structure] – Planar); (\*) corresponds to the process (ideal gas, 1 mol.L<sup>-1</sup>) → (ideal dilute solution, 1 mol.L<sup>-1</sup>).

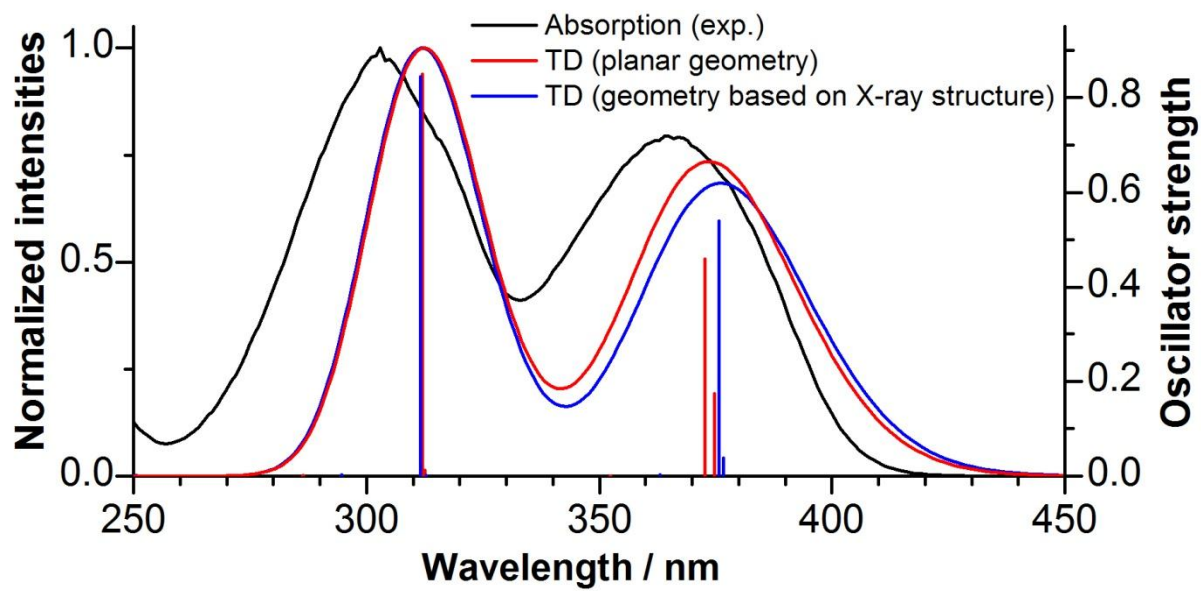


Fig. S20 Simulated electronic spectra (TD-DFT – B3LYP/6-31G(d,p)/PCM( $\text{CH}_2\text{Cl}_2$ ) of compound 5.

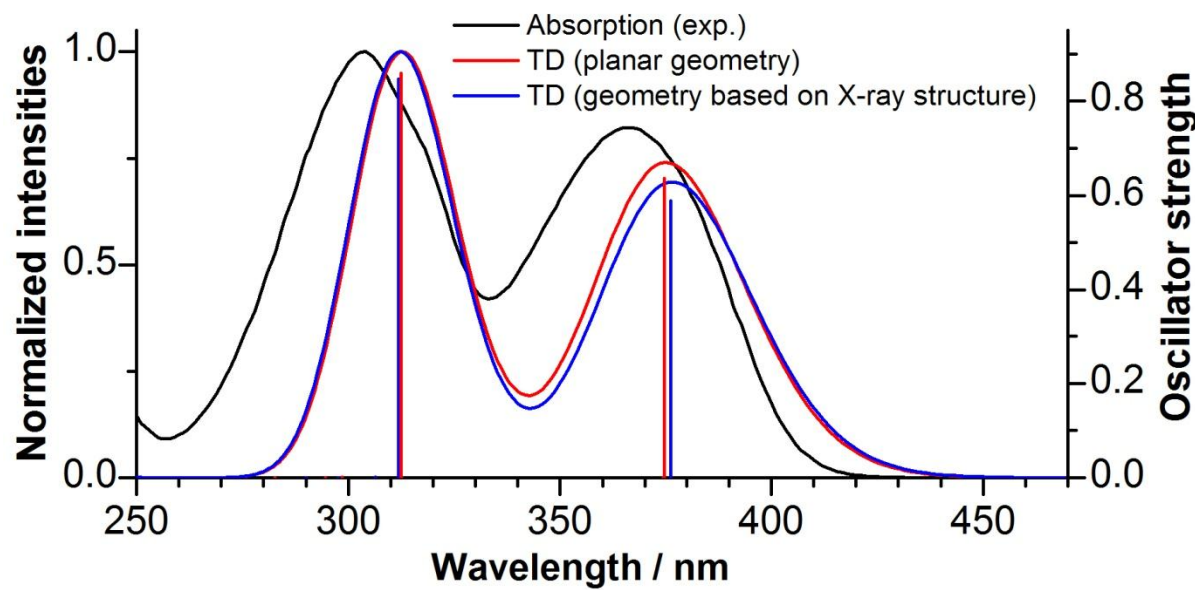
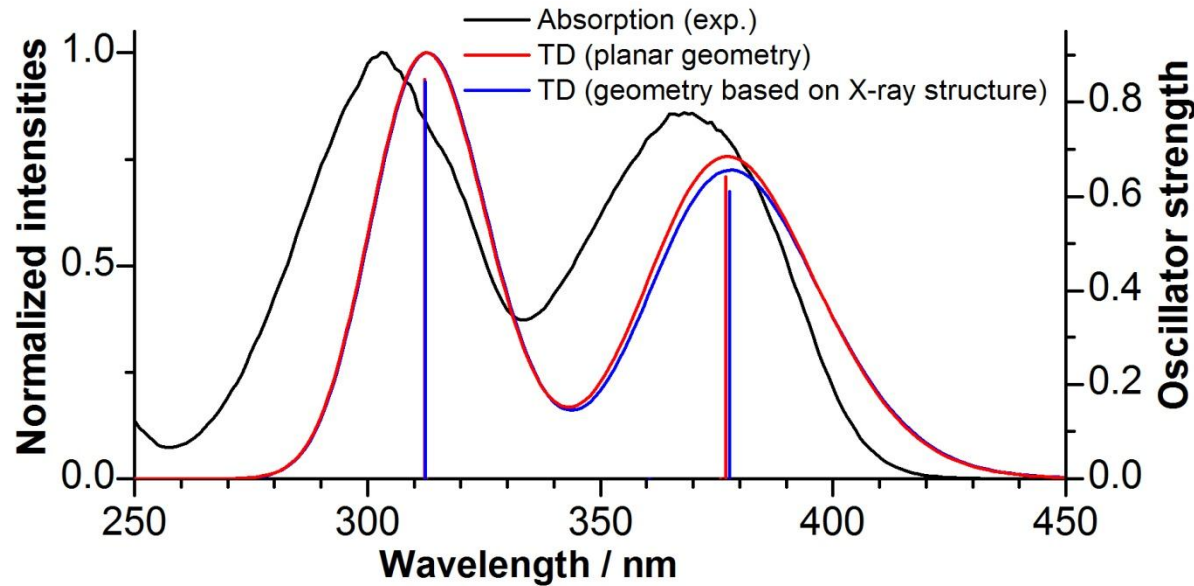
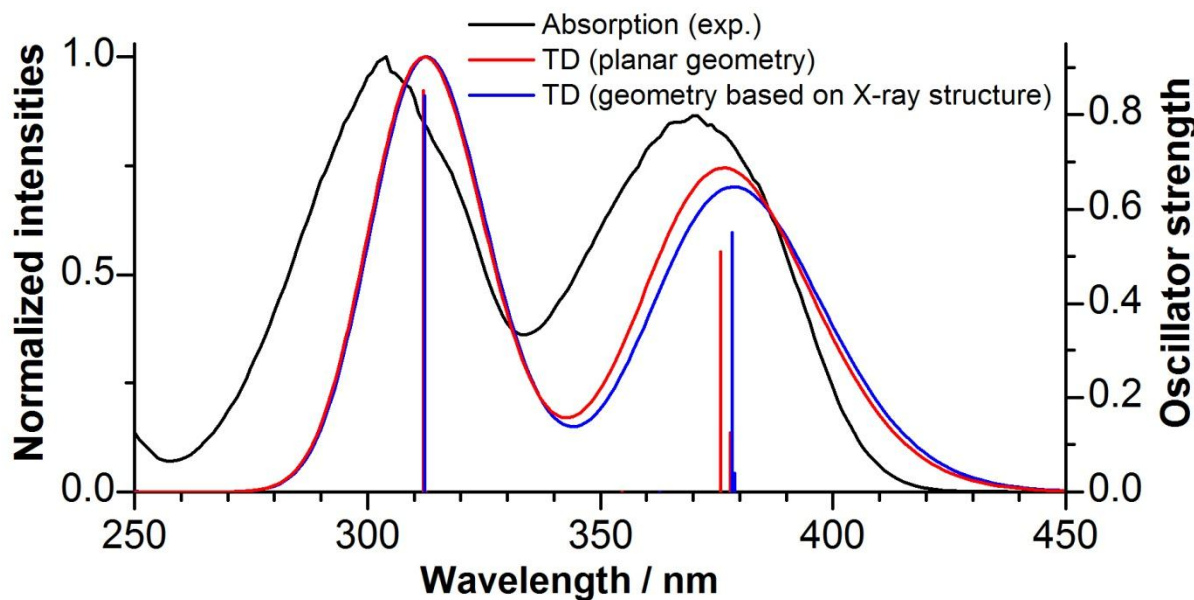


Fig. S21 Simulated electronic spectra (TD-DFT – B3LYP/6-31G(d,p)/PCM( $\text{CH}_2\text{Cl}_2$ ) of compound 6.



**Fig. S22** Simulated electronic spectra (TD-DFT – B3LYP/6-31G(d,p)/PCM( $\text{CH}_2\text{Cl}_2$ ) of compound **10**.



**Fig. S23** Simulated electronic spectra (TD-DFT – B3LYP/6-31G(d,p)/PCM( $\text{CH}_2\text{Cl}_2$ ) of compound **11**.

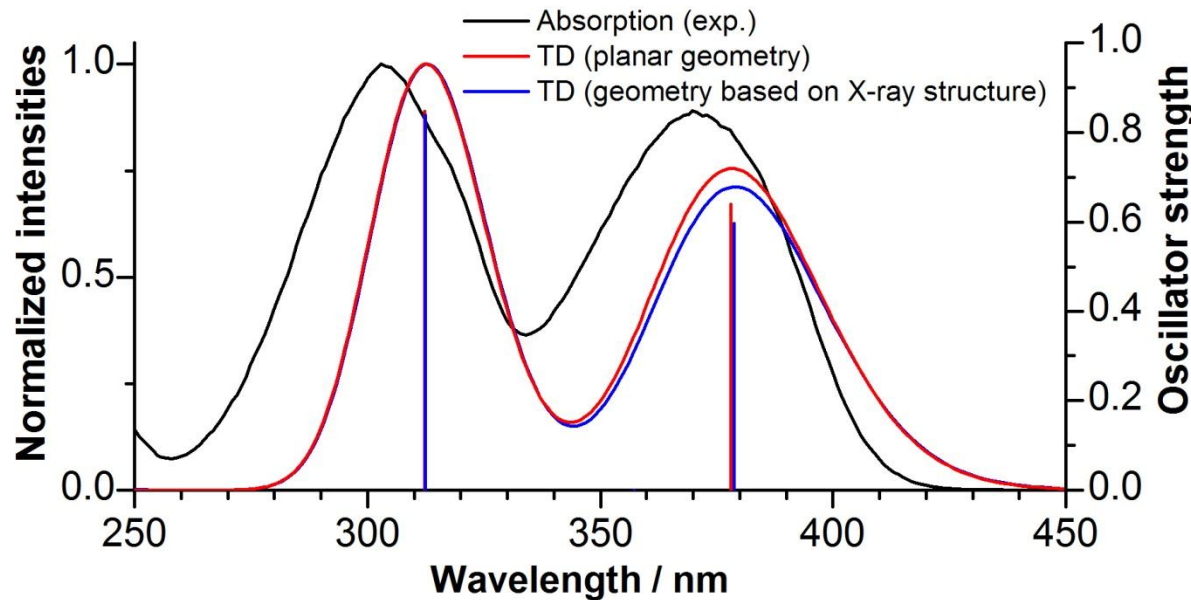


Fig. S24 Simulated electronic spectra (TD-DFT – B3LYP/6-31G(d,p)/PCM( $\text{CH}_2\text{Cl}_2$ ) of compound 12.

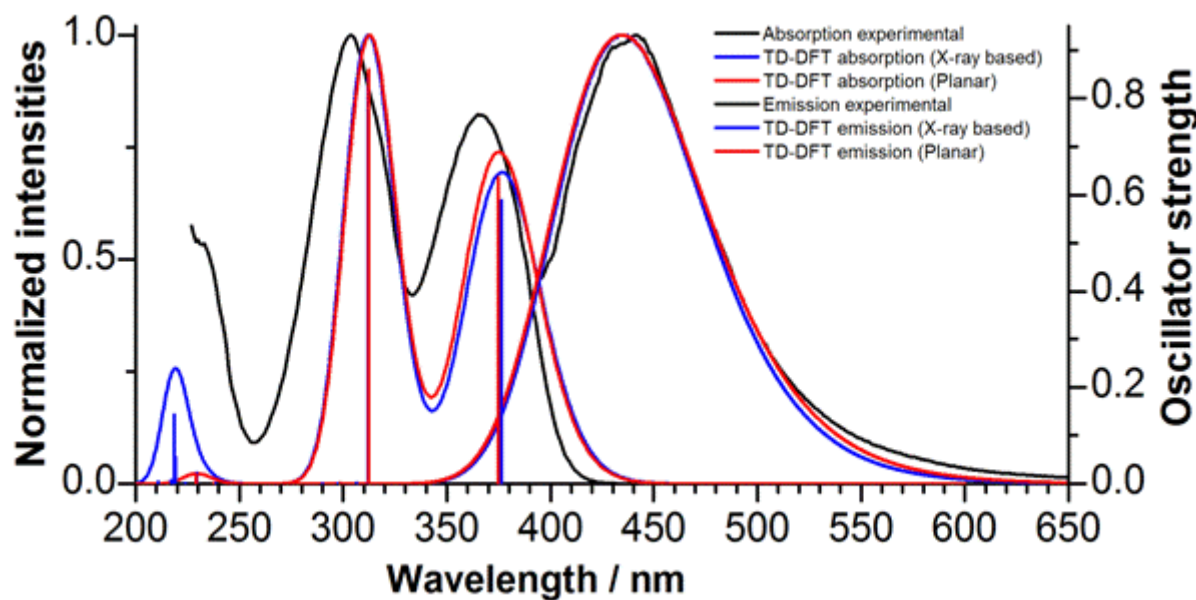


Fig. S25 Simulated absorption and emission spectra (TD-DFT – B3LYP/6-31G(d,p)/PCM( $\text{CH}_2\text{Cl}_2$ ) for the planar and X-ray geometry of compound 6 (structure obtained from CIF file).

**Table S5** TD-DFT main electronic transitions calculated by B3LYP/6-31G(d,p)/PCM(CH<sub>2</sub>Cl<sub>2</sub>) for the structures obtained from CIF files.

Comp.	$\lambda$ (exp.)	$\lambda$ (TD)	$f$	contributors	Assig.
				Major	Minor
<b>5</b>	365	376.7	0.039	H-1 → LUMO (40%) HOMO → L+1 (51%)	H-3 → LUMO (4%) H-2 → L+1 (4%)
		375.8	0.539	H-3 → L+1 (39%) HOMO → LUMO (51%)	H-3 → L+1 (5%) H-2 → LUMO (5%)
	303	311.5	0.844	H-3 → L+1 (42%) H-2 → LUMO (46%)	H-1 → L+1 (5%) HOMO → LUMO (5%)
<b>6</b>	366	376.3	0.589	H-1 → LUMO (44%) HOMO → L+1 (45%)	H-3 → LUMO (4%) H-2 → L+1 (4%)
	304	311.8	0.846	H-3 → LUMO (43%) H-4 → L+1 (46%)	H-1 → LUMO (5%) HOMO → L+1 (5%)
<b>10</b>	369	377.8	0.611	H-1 → L+1 (43%) HOMO → LUMO (47%)	H-3 → L+1 (4%) H-2 → LUMO (5%)
	303	312.5	0.843	H-3 → L+1 (44%) H-2 → LUMO (45%)	H-1 → L+1 (5%) HOMO → LUMO (5%)
<b>11</b>	369	378.9	0.389	H-1 → LUMO (47%) HOMO → L+1 (47%)	H-3 → L+1 (4%) H-2 → LUMO (4%)
		378.4	0.551	H-1 → L+1 (43%) HOMO → LUMO (47%)	H-3 → LUMO (7%) H-1 → L+1 (2%)
	304	312.3	0.840	H-3 → L+1 (44%) H-2 → LUMO (45%)	H-1 → L+1 (5%) HOMO → LUMO (5%)
<b>12</b>	371	378.8	0.597	H-1 → L+1 (44%) HOMO → LUMO (45%)	H-3 → L+1 (4%) H-2 → LUMO (3%)
	303	312.4	0.838	H-3 → L+1 (44%) H-2 → LUMO (45%)	H-1 → L+1 (5%) HOMO → LUMO (4%)

**Table S6** TD-DFT main electronic transitions calculated by B3LYP/6-31G(d,p)/PCM(CH<sub>2</sub>Cl<sub>2</sub>) for the fully planar structures with zig-zag arrangement of the spacers.

Comp.	$\lambda$ (exp.)	$\lambda$ (TD)	$f$	contributors	Assig.	
				Major	Minor	
<b>5</b>	365	374.8	0.1739	HOMO → LUMO (41%) H-1 → L+1 (35%)	H-3 → L+1 (4%) H-2 → LUMO (4%) H-1 → LUMO (7%) HOMO → L+1 (7%)	$\pi-\pi^*$
		372.8	0.4595	H-1 → LUMO (36%) HOMO → L+1 (42%)	H-3 → LUMO (4%) H-2 → L+1 (4%) H-1 → L+1 (5%) HOMO → LUMO (5%)	$\pi-\pi^*$
	303	312	0.849	H-3 → LUMO (38%) H-2 → L+1 (39%)	H-3 → L+1 (5%) H-2 → LUMO (5%) H-1 → LUMO (5%) HOMO → L+1 (5%)	$\pi-\pi^*$
<b>6</b>	366	374.8	0.6358	H-1 → L+1 (44%) HOMO → LUMO (45%)	H-3 → L+1 (5%) H-2 → LUMO (5%)	$\pi-\pi^*$
	303	312.4	0.8586	H-3 → L+1 (44%) H-2 → LUMO (44%)	H-1 → L+1 (5%) HOMO → LUMO (5%)	$\pi-\pi^*$
<b>10</b>	369	377.1	0.6419	H-1 → L+1 (44%) HOMO → LUMO (46%)	H-3 → L+1 (4%) H-2 → LUMO (4%)	$\pi-\pi^*$
	303	312.3	0.8483	H-3 → L+1 (44%) H-2 → LUMO (45%)	H-1 → L+1 (5%) HOMO → LUMO (5%)	$\pi-\pi^*$
<b>11</b>	369	377.9	0.1247	H-1 → L+1 (44%) HOMO → LUMO (47%)	H-3 → L+1 (4%) H-2 → LUMO (4%)	$\pi-\pi^*$
		375.9	0.5099	H-1 → LUMO (44%) HOMO → L+1 (46%)	H-3 → LUMO (5%) H-2 → L+1 (4%)	$\pi-\pi^*$
	303	311.9	0.8505	H-3 → LUMO (44%) H-2 → L+1 (45%)	H-1 → LUMO (5%) HOMO → L+1 (5%)	$\pi-\pi^*$
<b>12</b>	371	378.1	0.64	H-1 → LUMO (45%) HOMO → L+1 (46%)	H-3 → LUMO (4%) H-2 → L+1 (4%)	$\pi-\pi^*$
	303	312.3	0.8474	H-3 → LUMO (45%) H-2 → L+1 (45%)	H-1 → LUMO (5%) HOMO → L+1 (5%)	$\pi-\pi^*$

**Table S7.** The selected bond lengths (Å) obtained for the optimized structure (from CIF file) for the ground (GS) and excited (ES) states, as well as for the first and second reduced forms of compound **6**.

<b>Bond</b>	<b>GS(PCM)</b>	<b>ES(PCM)</b>	<b>GS<sup>a</sup>(PCM)</b>	<b>1<sup>st</sup> red. PCM</b>		<b>1<sup>st</sup> red. Vacuum</b>
				<b>Reduced side</b>	<b>Neutral side</b>	
C <sub>9</sub> -N <sub>10</sub>	1.165	1.173	1.165	1.177	1.165	1.170
C <sub>9'</sub> -N <sub>10'</sub>	1.164	1.171	1.165	1.175	1.165	1.169
C <sub>8</sub> -C <sub>9</sub>	1.430	1.414	1.430	1.410	1.430	1.423
C <sub>9</sub> -C <sub>8'</sub>	1.433	1.419	1.433	1.414	1.433	1.427
<b>C<sub>7</sub>-C<sub>8</sub></b>	<b>1.373</b>	<b>1.416</b>	<b>1.375</b>	<b>1.438</b>	<b>1.375</b>	<b>1.400</b>
C <sub>1</sub> -C <sub>7</sub>	1.442	1.445	1.441	1.420	1.441	1.433
<b>C<sub>1</sub>-C<sub>2</sub></b>	<b>1.413</b>	<b>1.391</b>	<b>1.414</b>	<b>1.427</b>	<b>1.415</b>	<b>1.420</b>
<b>C<sub>2</sub>-C<sub>3</sub></b>	<b>1.386</b>	<b>1.424</b>	<b>1.387</b>	<b>1.394</b>	<b>1.387</b>	<b>1.391</b>
C <sub>3</sub> -C <sub>4</sub>	1.399	1.396	1.401	1.398	1.401	1.397
C <sub>4</sub> -C <sub>5</sub>	1.393	1.397	1.394	1.409	1.394	1.403
C <sub>5</sub> -C <sub>6</sub>	1.400	1.410	1.401	1.390	1.402	1.394
<b>C<sub>1</sub>-C<sub>6</sub></b>	<b>1.430</b>	<b>1.457</b>	<b>1.432</b>	<b>1.445</b>	<b>1.432</b>	<b>1.437</b>
<b>C<sub>6</sub>-O<sub>11</sub></b>	<b>1.351</b>	<b>1.332</b>	<b>1.352</b>	<b>1.373</b>	<b>1.352</b>	<b>1.368</b>
O <sub>11</sub> -C <sub>12</sub>	1.435	1.447	1.439	1.426	1.439	1.423

<sup>a</sup>Calculated at the B3-LYP/6-31+G (d,p)/PCM(CH<sub>2</sub>Cl<sub>2</sub>) level. The variation in the angles is not significant, it was not observed changes large than 2 degrees.

**Table S8.** The selected bond lengths (Å) obtained from the optimized structure (using the planar geometry) for the ground (GS) and excited (ES) states, as well as for the first and second reduced forms of compound **6**.

<b>Bond</b>	<b>GS(PCM)</b>	<b>ES(PCM)</b>	<b>GS<sup>a</sup>(PCM)</b>	<b>1<sup>st</sup> red. PCM</b>		<b>1<sup>st</sup> red. Vacuum</b>
				<b>Reduced side</b>	<b>Neutral side</b>	
C <sub>9</sub> -N <sub>10</sub>	1.165	1.173	1.165	1.176	1.165	1.170
C <sub>9'</sub> -N <sub>10'</sub>	1.164	1.172	1.165	1.175	1.165	1.169
C <sub>8</sub> -C <sub>9</sub>	1.430	1.414	1.430	1.410	1.430	1.423
C <sub>9</sub> -C <sub>8'</sub>	1.433	1.419	1.433	1.414	1.433	1.427
<b>C<sub>7</sub>-C<sub>8</sub></b>	<b>1.373</b>	<b>1.416</b>	<b>1.374</b>	<b>1.438</b>	<b>1.374</b>	<b>1.400</b>
C <sub>1</sub> -C <sub>7</sub>	1.442	1.444	1.442	1.420	1.442	1.433
<b>C<sub>1</sub>-C<sub>2</sub></b>	<b>1.413</b>	<b>1.392</b>	<b>1.414</b>	<b>1.427</b>	<b>1.415</b>	<b>1.420</b>
<b>C<sub>2</sub>-C<sub>3</sub></b>	<b>1.386</b>	<b>1.424</b>	<b>1.388</b>	<b>1.393</b>	<b>1.387</b>	<b>1.391</b>
C <sub>3</sub> -C <sub>4</sub>	1.399	1.396	1.401	1.398	1.401	1.397
C <sub>4</sub> -C <sub>5</sub>	1.393	1.396	1.394	1.409	1.394	1.403
C <sub>5</sub> -C <sub>6</sub>	1.399	1.409	1.400	1.389	1.400	1.393
C <sub>1</sub> -C <sub>6</sub>	1.431	1.457	1.432	1.444	1.432	1.436
<b>C<sub>6</sub>-O<sub>11</sub></b>	<b>1.353</b>	<b>1.334</b>	<b>1.354</b>	<b>1.375</b>	<b>1.354</b>	<b>1.370</b>
O <sub>11</sub> -C <sub>12</sub>	1.432	1.442	1.435	1.424	1.436	1.422

<sup>a</sup>Calculated at the B3-LYP/6-31+G (d,p)/PCM(CH<sub>2</sub>Cl<sub>2</sub>) level.

**Table S9** The computed Mulliken ( $q_{Mull.}$ ) charges and spin densities for the different states of compound **6**, using the optimized structure obtained from CIF file.

Atom	GS	ES	GS <sup>a</sup>	1 <sup>st</sup> red. PCM			1 <sup>st</sup> red. Vacuum	
	S <sub>0</sub>	S <sub>1</sub>	S <sub>0</sub>	$q_{Mull}$ Reduced side	$q_{Mull}$ Neutral side	Spin	$q_{Mull}$	spin
C <sub>1</sub>	<b>0.046</b>	<b>0.108</b>	<b>0.812</b>	<b>0.628</b>	<b>0.810</b>	<b>-0.156</b>	<b>0.713</b>	<b>-0.060</b>
C <sub>2</sub>	-0.123	-0.153	-0.583	-0.664	-0.588	0.293	-0.600	0.144
C <sub>3</sub>	-0.101	-0.057	-0.402	-0.395	-0.393	-0.128	-0.370	-0.064
C <sub>4</sub>	-0.089	-0.104	-0.782	-0.897	-0.778	0.276	-0.815	0.144
C <sub>5</sub>	-0.134	-0.101	-0.771	0.754	0.776	-0.110	0.741	-0.052
C <sub>6</sub>	0.346	0.341	-0.104	0.035	-0.122	0.105	-0.021	0.047
C <sub>7</sub>	<b>-0.046</b>	<b>-0.142</b>	<b>0.554</b>	<b>0.297</b>	<b>0.538</b>	<b>0.554</b>	<b>0.413</b>	<b>0.247</b>
C <sub>8</sub>	0.085	0.062	0.953	0.812	0.955	0.110	0.842	0.071
C <sub>9</sub>	0.320	0.273	-0.799	-0.665	-0.793	-0.066	-0.760	-0.038
C <sub>9'</sub>	0.298	0.264	-0.162	-0.114	-0.144	-0.028	-0.124	-0.018
N <sub>10</sub>	-0.535	-0.576	-0.545	-0.698	-0.547	0.105	-0.553	0.055
N <sub>10'</sub>	-0.516	-0.551	-0.560	-0.697	-0.560	0.074	-0.553	0.040
O <sub>11</sub>	<b>-0.532</b>	<b>-0.451</b>	<b>-0.327</b>	<b>-0.358</b>	<b>-0.327</b>	<b>0.011</b>	<b>-0.321</b>	<b>0.005</b>
C <sub>12</sub>	0.024	0.001	0.554	0.602	0.562	0.002	0.596	0.001

<sup>a</sup>Calculated at the B3 LYP/6-31+G (d,p)/PCM(CH<sub>2</sub>Cl<sub>2</sub>) level.

**Table S10** The computed Mulliken ( $q_{Mull.}$ ) charges and spin densities for the different states of compound **6** on planar geometry.

Atom	GS	ES	GS <sup>a</sup>	1 <sup>st</sup> red. PCM			1 <sup>st</sup> red. Vacuum	
	S <sub>0</sub>	S <sub>1</sub>	S <sub>0</sub>	Reduced side	Neutral side	Spin		
C <sub>1</sub>	<b>0.049</b>	<b>0.112</b>	<b>0.744</b>	<b>0.629</b>	<b>0.748</b>	<b>-0.159</b>	<b>0.684</b>	<b>-0.062</b>
C <sub>2</sub>	-0.124	-0.155	-0.240	-0.315	-0.238	0.254	-0.264	0.123
C <sub>3</sub>	-0.100	-0.055	-0.571	-0.550	-0.572	-0.112	-0.535	-0.056
C <sub>4</sub>	-0.089	-0.104	-0.411	-0.510	-0.407	0.259	-0.453	0.135
C <sub>5</sub>	-0.133	-0.101	0.092	0.121	0.091	-0.096	0.092	-0.045
C <sub>6</sub>	0.346	0.340	0.103	0.148	0.096	0.123	0.147	0.056
C <sub>7</sub>	<b>-0.045</b>	<b>-0.140</b>	<b>0.537</b>	<b>0.251</b>	<b>0.538</b>	<b>0.552</b>	<b>0.375</b>	<b>0.248</b>
C <sub>8</sub>	0.086	0.064	0.832	0.668	0.827	0.116	0.720	0.074
C <sub>9</sub>	0.323	0.278	-0.610	-0.525	-0.611	-0.053	-0.594	-0.032
C <sub>9'</sub>	0.298	0.264	-0.251	-0.162	-0.250	-0.035	-0.212	-0.021
N <sub>10</sub>	-0.535	-0.577	-0.546	-0.698	-0.548	0.106	-0.553	0.056
N <sub>10'</sub>	-0.515	-0.549	-0.563	-0.699	-0.563	0.074	-0.555	0.040
O <sub>11</sub>	<b>-0.542</b>	<b>-0.461</b>	<b>-0.364</b>	<b>-0.398</b>	<b>-0.364</b>	<b>0.011</b>	<b>-0.370</b>	<b>0.005</b>
C <sub>12</sub>	0.027	0.005	0.109	0.163	0.109	0.002	0.129	0.001

<sup>a</sup>Calculated at the B3 LYP/6-31+G (d,p)/PCM(CH<sub>2</sub>Cl<sub>2</sub>) level.

**Table S11** The computed APT charges for the different states of compound **6**, using the optimized structure obtained from CIF file.

	GS (PCM)	GS <sup>a</sup> (PCM)	1 <sup>st</sup> red. PCM		1 <sup>st</sup> red. Vacuum
Atom	S <sub>0</sub>	S <sub>0</sub>	Reduced side	Neutral side	
C <sub>1</sub>	<b>-0.624</b>	<b>-0.666</b>	<b>0.197</b>	<b>-0.667</b>	<b>0.556</b>
C <sub>2</sub>	0.171	0.181	-0.159	0.182	-0.474
C <sub>3</sub>	-0.417	-0.457	0.005	-0.460	0.112
C <sub>4</sub>	0.271	0.269	-0.256	0.271	-0.647
C <sub>5</sub>	-0.246	-0.270	0.003	-0.269	0.439
C <sub>6</sub>	0.890	0.933	0.541	0.934	-0.277
C <sub>7</sub>	<b>0.863</b>	<b>0.921</b>	<b>0.243</b>	<b>0.923</b>	<b>1.326</b>
C <sub>8</sub>	-0.482	-0.532	-0.999	-0.534	-1.779
C <sub>9</sub>	0.300	0.341	0.722	0.344	1.715
C <sub>9'</sub>	0.432	0.501	1.032	0.499	-0.390
N <sub>10</sub>	-0.461	-0.503	-0.916	-0.507	-1.470
N <sub>10'</sub>	-0.542	-0.604	-1.078	-0.603	-0.055
O <sub>11</sub>	-1.136	-1.165	-1.155	-1.165	0.291
C <sub>12</sub>	0.765	0.756	0.739	0.756	0.019

<sup>a</sup>Calculated at the B3 LYP/6-31+G (d,p)/PCM(CH<sub>2</sub>Cl<sub>2</sub>) level.

**Table S12** The computed APT charges for the different states of compound **6** on planar geometry.

	GS	GS <sup>a</sup>	1 <sup>st</sup> red. PCM		1 <sup>st</sup> red. Vacuum
Atom	S <sub>0</sub>	S <sub>0</sub>	Reduced side	Neutral side	
C <sub>1</sub>	<b>-0.625</b>	<b>-0.661</b>	<b>0.203</b>	<b>-0.664</b>	<b>0.113</b>
C <sub>2</sub>	0.167	0.175	-0.163	0.176	-0.454
C <sub>3</sub>	-0.416	-0.451	0.001	-0.454	0.131
C <sub>4</sub>	0.271	0.265	-0.259	0.267	-0.521
C <sub>5</sub>	-0.244	-0.269	0.007	-0.268	0.266
C <sub>6</sub>	0.890	0.928	0.533	0.930	0.011
C <sub>7</sub>	<b>0.863</b>	<b>0.917</b>	<b>0.238</b>	<b>0.921</b>	<b>2.318</b>
C <sub>8</sub>	-0.480	-0.522	-0.995	-0.527	-2.716
C <sub>9</sub>	0.298	0.334	0.717	0.337	1.906
C <sub>9'</sub>	0.429	0.496	1.030	0.498	-0.089
N <sub>10</sub>	-0.460	-0.499	-0.911	-0.502	-1.651
N <sub>10'</sub>	-0.538	-0.660	-1.075	-0.600	-0.283
O <sub>11</sub>	<b>-1.140</b>	<b>-1.164</b>	<b>-1.154</b>	<b>-1.166</b>	<b>0.417</b>
C <sub>12</sub>	0.770	0.762	0.745	0.762	-0.178

<sup>a</sup>Calculated at the B3 LYP/6-31+G (d,p)/PCM(CH<sub>2</sub>Cl<sub>2</sub>) level.

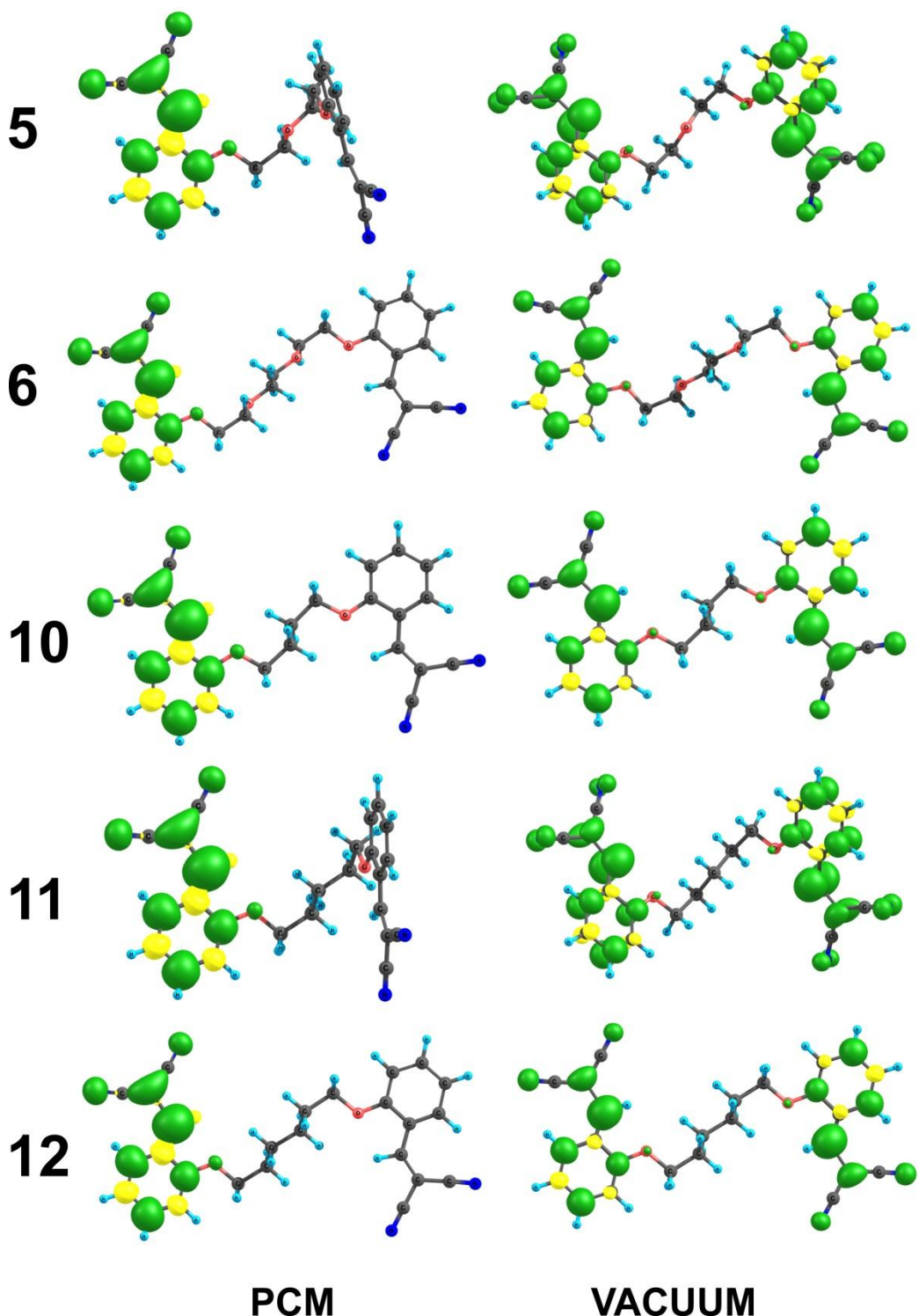


**Fig. S26** The spin density distributions of the first reduction. The structures were optimized from CIF file.

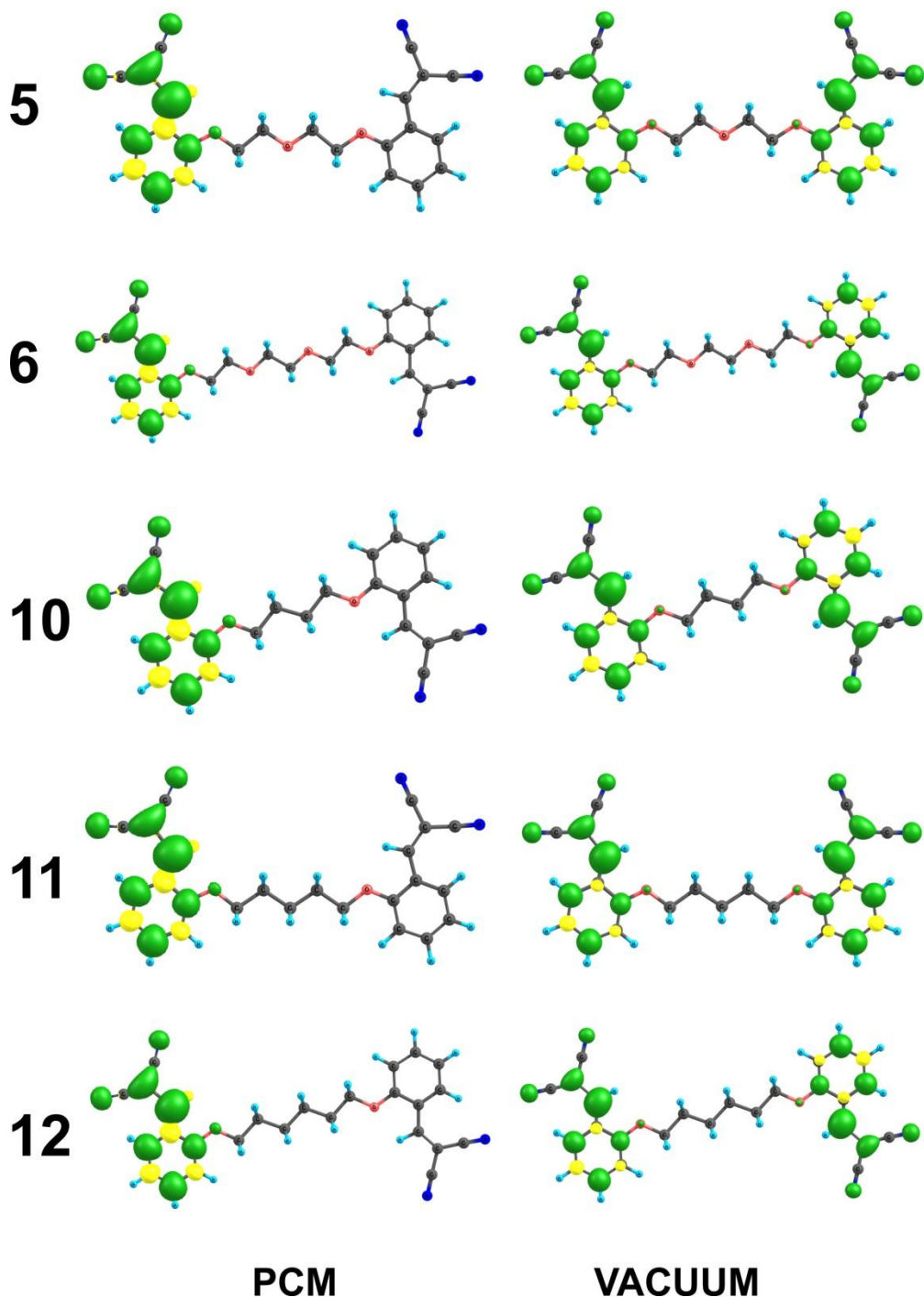


**Fig. S27** The spin density distributions of the first reduction using the planar geometry.

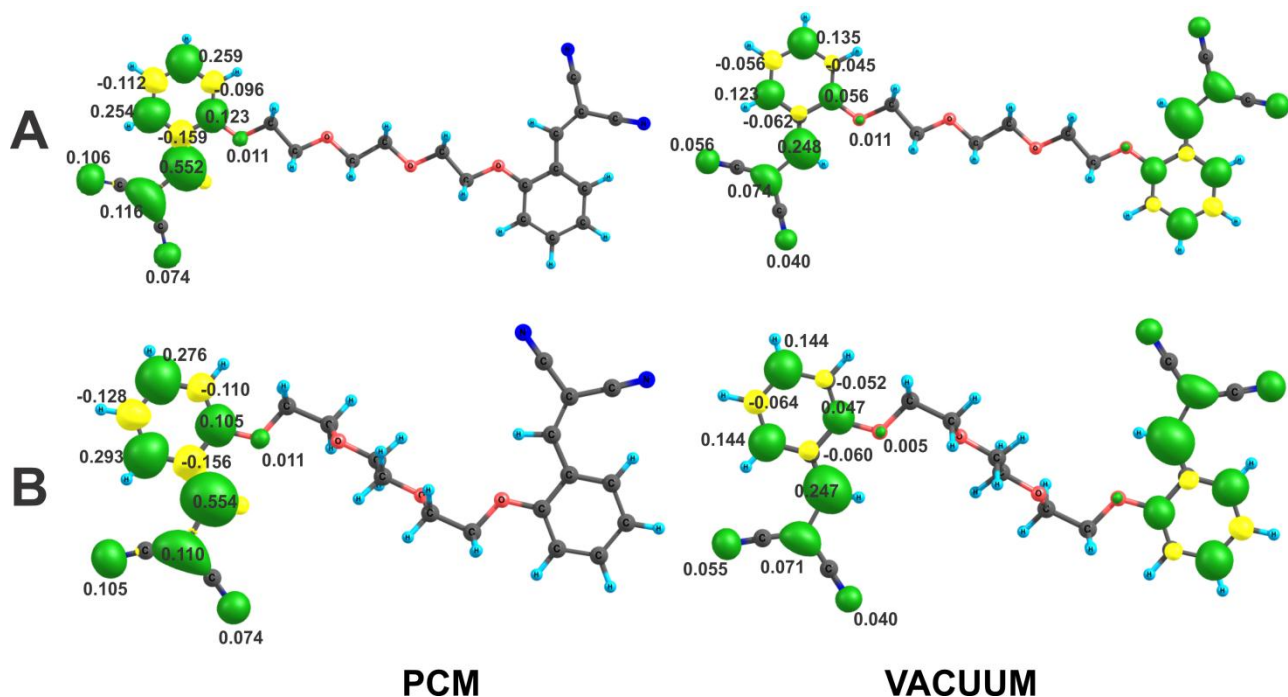


**Fig. S28** The spin density distributions of the first reduction of compound 6, forming an anion and the second reduction of compound 6, forming a di-anion. (A) Planar geometry and (B) structure obtained from the CIF files.

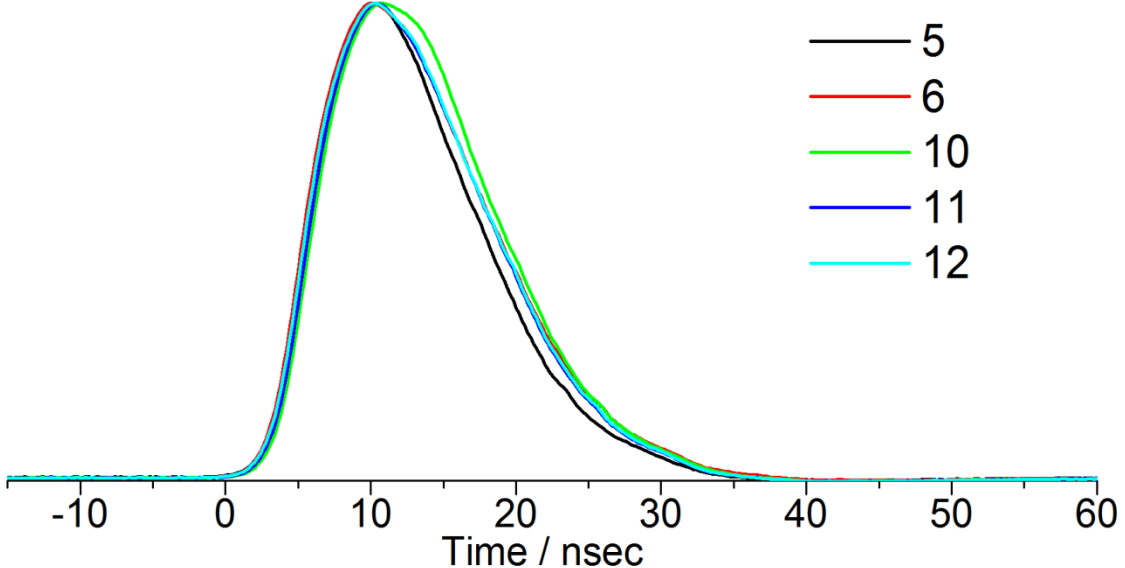


**Fig. S29** Lifetime decay waveforms of the examined dicyanomethylene compounds in  $\text{CH}_2\text{Cl}_2$ .

1 J. R. Pliego, J. M. Riveros, *Phys. Chem. Chem. Phys.*, 2002, **4**, 1622.

2 A. Ben-Naim, *J. Phys. Chem.*, 1978, **82**, 792.